International Journal for Parasitology xxx (2016) xxx–xxx

Contents lists available at ScienceDirect

International Journal for Parasitology

journal homepage: www.elsevier.com/locate/ijpara

Automated parasite faecal egg counting using fluorescence labelling, smartphone image capture and computational image analysis

Paul Slusarewicz [a,b,*], Stefanie Pagano [a,b], Christopher Mills [a,b], Gabriel Popa [c], K. Martin Chow [c], Michael Mendenhall [c], David W. Rodgers [c], Martin K. Nielsen [b]

[a] MEP Equine Solutions, 3905 English Oak Circle, Lexington, KY 40514, USA
[b] M.H. Gluck Equine Research Center, Department of Veterinary Science, University of Kentucky, Lexington, KY, USA
[c] Department of Molecular & Cellular Biochemistry, University of Kentucky, Lexington, KY, USA

ARTICLE INFO

Article history:
Received 11 December 2015
Received in revised form 23 February 2016
Accepted 25 February 2016
Available online xxxx

Keywords:
Egg count
Chitin
Fluorescence
Smartphone
Image analysis
Strongyle
Ascarid
Equine

ABSTRACT

Intestinal parasites are a concern in veterinary medicine worldwide and for human health in the developing world. Infections are identified by microscopic visualisation of parasite eggs in faeces, which is time-consuming, requires technical expertise and is impractical for use on-site. For these reasons, recommendations for parasite surveillance are not widely adopted and parasite control is based on administration of rote prophylactic treatments with anthelmintic drugs. This approach is known to promote anthelmintic resistance, so there is a pronounced need for a convenient egg counting assay to promote good clinical practice. Using a fluorescent chitin-binding protein, we show that this structural carbohydrate is present and accessible in shells of ova of strongyle, ascarid, trichurid and coccidian parasites. Furthermore, we show that a cellular smartphone can be used as an inexpensive device to image fluorescent eggs and, by harnessing the computational power of the phone, to perform image analysis to count the eggs. Strongyle egg counts generated by the smartphone system had a significant linear correlation with manual McMaster counts ($R^2 = 0.98$), but with a significantly lower coefficient of variation ($P = 0.0177$). Furthermore, the system was capable of differentiating equine strongyle and ascarid eggs similar to the McMaster method, but with significantly lower coefficients of variation ($P < 0.0001$). This demonstrates the feasibility of a simple, automated on-site test to detect and/or enumerate parasite eggs in mammalian faeces without the need for a laboratory microscope, and highlights the potential of smartphones as relatively sophisticated, inexpensive and portable medical diagnostic devices.
© 2016 Australian Society for Parasitology Inc. Published by Elsevier Ltd. All rights reserved.

1. Introduction

Intestinal parasite infections are concerns in both humans and animals. Thus the World Health Organization (WHO) has recommended the use of faecal egg counts (FECs) to monitor schistosomiasis and soil-transmitted helminth infections in humans in developing countries (WHO, 2006). Similarly, the World Association for the Advancement of Veterinary Parasitology (WAAVP) recommends FECs for assessment of intestinal parasite infection intensity and anthelmintic efficacy in livestock (Wood et al., 1995). Monitoring FEC levels is widely recommended in targeted selective therapy control programs in both ruminants and equines (Kenyon et al., 2009; Nielsen et al., 2014). These recommendations make huge demands on current FEC techniques, which require microscopes, other laboratory equipment and trained personnel, and are thus rarely performed on-site. As a result, egg counting has been historically under utilised as a diagnostic and monitoring tool in human and animal parasite control, and the consequence has been a tendency to address parasite infection by rote prophylactic treatment (Vercruysse et al., 2012; Leathwick and Besier, 2014; Robert et al., 2015). The resulting evolution of anthelmintic resistance is now a global problem in parasite populations present across all domesticated animal species (Kaplan, 2004; Howell et al., 2008; Cezar et al., 2010; da Cruz et al., 2010; Peregrine et al., 2014) and a growing concern in humans (Alum et al., 2010; Vercruysse et al., 2011). This trend is all the more worrying due to the slow pace of development of new anthelmintic drug classes (Kaplan, 2004).

Despite this burgeoning need and the development of sophisticated diagnostics in other areas of human and veterinary medicine, egg counting has remained relatively unchanged since the first method descriptions almost a century ago (Stoll, 1930; Gordon

* Corresponding author at: MEP Equine Solutions, 3905 English Oak Circle, Lexington, KY 40514, USA. Tel.: +1 512 818 8470.
E-mail address: pslusarewicz@mepequinesolutions.com (P. Slusarewicz).

http://dx.doi.org/10.1016/j.ijpara.2016.02.004
0020-7519/© 2016 Australian Society for Parasitology Inc. Published by Elsevier Ltd. All rights reserved.

Please cite this article in press as: Slusarewicz, P., et al. Automated parasite faecal egg counting using fluorescence labelling, smartphone image capture and computational image analysis. Int. J. Parasitol. (2016), http://dx.doi.org/10.1016/j.ijpara.2016.02.004

and Whitlock, 1939), although useful innovation has been introduced by enlarging flotation chamber volumes to improve sensitivity (Cringoli et al., 2004; Levecke et al., 2012; Barda et al., 2013), exploration of alternative flotation solutions (Cringoli et al., 2004; Vadlejch et al., 2011), and by developing flotation chamber adaptors to allow direct centrifugation-enhanced flotation (Cringoli et al., 2010). Recent work has illustrated the potential for utilising novel imaging modalities and using computational image analysis to identify eggs and generate parasite FECs, and this technological field is rapidly evolving (Yang et al., 2001; Castanon et al., 2007; Mes et al., 2007; Dogantekin et al., 2008; Ghazali et al., 2013; Linder et al., 2013; Suzuki et al., 2013; Cooke et al., 2015).

One alternative approach to the FEC might involve using an accessible universal egg marker (UEM) to serve as a target for detection. Unfortunately, little has been done to elucidate the molecular composition of egg surfaces of clinically relevant parasites, and what little has been done has yielded scant specific information (Wharton, 1983; Quiles et al., 2006). Nevertheless, chitin has been identified in many helminth egg types (Bird and McClure, 1976; Wharton, 1983; Perry and Trett, 1986; Burgwyn et al., 2003) and this, coupled to the rationalisation that such a structural carbohydrate is much more likely to have been evolutionarily conserved than a protein, led us to postulate that chitin could serve as a UEM on all helminth egg surfaces and thus form the basis of a test for total parasite egg count.

Furthermore, due to their low cost and ubiquity, there is currently intense interest in harnessing the optics and computational power of smartphones to produce affordable and convenient analytical instruments and diagnostic devices for use outside the laboratory (Zhu et al., 2013), including in the area of parasitology (Bogoch et al., 2013, 2016; Ephraim et al., 2015; Sowerby et al., 2016), although none have yet been commercialised. We therefore sought to eliminate the need for a laboratory microscope and laborious manual specimen examination by simplifying and automating FECs via coupling fluorescent egg staining to smartphone-based imaging and computational shape recognition (United States patent application #2015029309).

2. Materials and methods

2.1. Protein cloning, expression and labelling

The chitin binding domain (CBD) from *Bacillus circulans* chitinase A1 that was used to detect parasite eggs was produced as a hexahistidine (his6 tag)-intein-CBD fusion protein using the plasmid pTXB1 (New England Biolabs, Ipswich, MA, USA). pTXB1 was digested with *Not*I and *Nhe*I, and ligated to a his6-encoding adaptor made by annealing two synthetic oligonucleotides (5′-CTAGCCAT CATCACCATCACCAC-3′ and 5′-GGCCGTGGTGATGGTGATGATGG-3′) . The resultant construct was confirmed by DNA sequencing and transfected into the BL21-CodonPlus (DE3)-RP *Escherichia coli* strain (Agilent Technologies, Santa Clara, CA, USA). Cells were grown in lysogeny broth (LB) medium at 37 °C to an O.D. 600 of approximately 1.5 in a 10 L fermenter (New Brunswick Scientific, Enfield, CT, USA). Transcription was induced by addition of 1 mM isopropyl-1-thio-β-D-galacto-pyranoside after lowering the growth temperature to 16 °C. After 12–18 h, cells were pelleted and suspended in 50 mM sodium phosphate, pH 8.0, lysed by sonication after addition of phenylmethylsulfonyl fluoride to 1 mM and lysozyme to 1 mg/ml, and debris cleared by centrifugation at 20,000*g* for 60 min. The his6 tag was used for purification on Ni-NTA agarose with a ratio of 2.5 ml of settled resin/L of original culture. Protein binding and subsequent washes with buffer containing sodium chloride up to 1.0 M were done on a small gravity feed column. Protein was eluted with 200 mM imidazole, dialyzed against PBS, and concentrated using a centrifugal concentrator to 11 mg/ml. For labelling, a 4 mg/ml solution of CBD in 100 mM sodium bicarbonate, pH 10, was incubated in the presence of 500 μM hydroxysuccinimide-fluorescein added in DMSO. Samples were incubated in the dark at room temperature for 60 min, and then NH_4Cl added to 10 mM followed by a further 60 min incubation. Unreacted fluorophore was removed by sequential centrifugal concentration and dilution with PBS until the filtrate was colourless.

2.2. Faecal processing

Faecal samples were collected fresh from horses, goats, sheep and cattle present at the University of Kentucky Maine Chance Research Farm, USA. Furthermore, canine samples were obtained from a local shelter and feline samples from a local veterinary practice. All samples were stored in airtight containers and kept refrigerated until analysis.

Five grams of faeces was suspended in 45 ml of flotation solution (350 g of glucose and 175 g of sodium chloride in water to a final volume of 1 L, specific gravity 1.26 g/ml) in a fill-FLOTAC vessel (Barda et al., 2013). The filter (~1 mm aperture) in the fill-FLOTAC served as a primary filter. After expulsion, the slurry was used either for egg staining or for manual counting, after gentle agitation immediately prior to sampling to evenly suspend the eggs. In the latter case, 0.5 ml of the fill-FLOTAC filtrate was loaded into each McMaster counting chamber, left to sit for 5 min, and eggs within the grid (volume = 0.15 ml) were then counted manually at 40× magnification.

Alternatively, to stain eggs for subsequent imaging in a McMaster counting chamber, 5 ml of fill-FLOTAC slurry was loaded onto a stack of cell strainers fitted with membranes of varying pore sized (pluriSelect Life Science, Leipzig, Germany) consisting of a 200 μm (for ascarid-containing samples) or a 90 μm unit atop a 27 μm membrane. The filters were attached to a 50 ml disposable centrifuge tube via the manufacturer's collar, which contained a vacuum port, and the material drawn through using a 50 ml syringe.

Material on the 27 μm membrane was stained using 1 ml of 60 μg/ml fluorescent (F)-CBD in 1x blocking buffer (Vector Laboratories, Burlingame, CA, USA) in PBS for 2 min, and rinsed with three consecutive 5 ml washes of PBS. Post-staining, eggs were recovered from the filter with 0.5 ml of PBS using a pipette and five to 10 cycles of ejection and aspiration, and placed under a glass cover slip or into an etched McMaster chamber. In control experiments, F-CBD was pretreated by either heating at 95 °C for 5 min or incubating with 1x chitin hydrolysate (Vector Laboratories) in PBS.

In the case of imaging on filters, faecal suspensions in faecal slurry in flotation solution were passed though the fill-FLOTAC and a number of 200 μm or 90 μm filters and pooled, then 3 ml of suspension was loaded onto each filter unit. Samples were bleached, stained and washed as described above.

In eggs of the free-living nematode *Caenorhabditis elegans*, chitin can only be accessed after bleaching (Zhang et al., 2005), which presumably compromises the outer vitelline layer (Olson et al., 2012). Therefore, in most cases, faecal samples were bleached with 1% sodium hypochlorite for 1 or more minutes and then washed with three 5 ml rinses of PBS prior to staining. In the case of equine ascarids and *Trichuris* spp. eggs, bleaching was conducted for 5 min, including equine samples containing mixtures of ascarids and strongyles.

2.3. Imaging

Stained eggs in a McMaster chamber were imaged either with an Eclipse Ti fluorescence microscope or with a smartphone (Apple iPhone 5s, Apple Inc., Cupertino, CA, USA; Sony Experia Z3, Sony Corporation, New York, NY, USA; Nokia Lumia 1020, Nokia

Please cite this article in press as: Slusarewicz, P., et al. Automated parasite faecal egg counting using fluorescence labelling, smartphone image capture and computational image analysis. Int. J. Parasitol. (2016), http://dx.doi.org/10.1016/j.ijpara.2016.02.004

Solutions and Networks, Espoo, Finland). Output resolutions of the cameras were 3264 × 2448 (iPhone 5s), 5248 × 3936 (Experia z3) and 7152 × 5360 (Lumia 1020). In the case of smartphones, images were generated by placing the McMaster slide containing the sample in a gel fluorescence imaging device (PrepOne Sapphire, EmbiTec, San Diego, CA, USA; Fig. 1A). This device contains a bank of blue light emitting diodes that encompass the excitation energy wavelengths of fluorescein and is supplied with a sheet of clear orange acrylic that acts as an emission filter. The iPhone 5s was fitted with a 7× macro lens (Olloclip, Huntington Beach, CA, USA) and positioned so that the McMaster chamber almost filled the shorter dimension of the image sensor (Fig. 1C).

In the case of epifluorescent iPhone imaging, a device was constructed that contained a battery powered circuit board containing a hole surrounded by a concentric ring of eight blue light emitting diodes (LEDs) (Nichia NESB157AT). An optical tube containing a 25 mm × 25 Focal Length (FL) achromat lens (Edmund Optics, Barrington, NJ, USA) and a 525 nm highpass filter was passed though the circuit board and screwed into the body of the unit at a position where it would be juxtaposed with the phone lens once it was in place on the cradle. The circuit board was sealed with a cover containing a screw-mount positioned below the LED array and onto which a sample-containing membrane filter could be attached for imaging.

We also designed a custom filter housing for use with the units. This consisted of two halves that could be screwed together and sandwiched a 368 µm stainless steel support mesh overlaid with a 25 mm diameter 20 µm pore nylon filter membrane (Millipore, Darmstadt, Germany). The internal diameter of the filter unit was 22 mm. The filter unit had screw-threads above to facilitate attachment to the imaging unit and below to attach to a standard disposable 50 ml centrifuge tube. The distance of the filter from the camera was chosen so that the projected image of the filter filled the shortest dimension of the image sensor. The filter unit also contained a luer lock attachment to facilitate suction with a syringe once it was attached to the tube.

2.4. Image analysis

In morphometric studies, two faecal samples were divided and either resuspended in flotation solution, placed into McMaster chambers and multiple microscopic bright field photographs taken at 100×, or processed by bleaching and staining as described in Section 2.2 and then photographed in fluorescence mode at the same magnification. Scale bars were burned onto images using the microscope software. The resulting images were imported into ImageJ software (National Institutes of Health (NIH), Bethesda, MD, USA) and the scale set using the in-built Set Scale function in conjunction with the scale bar in each image. Thresholds for each were set until each egg (although not necessarily the center) was completely outlined. The software then computed the best-fit ellipse for each egg and returned values for area, axial lengths and aspect ratio (AR). In cases where eggs were touching faecal debris that could not be isolated by thresholding, debris was eliminated digitally using software (Photoshop, Adobe Systems Inc., San Jose, CA, USA) prior to analysis. The total number of eggs measured for each group is shown in Table 1.

In initial studies using the pictures of fluorescing eggs in McMaster chambers, images from the iPhone were exported to a laptop PC running Windows 8.1 and processed with Photoshop CS6 using the curves and threshold functions. Firstly, the image was cropped to retain only the grid of the counting chamber. Then, using the curves function, the X axis values of the RGB channel were set to 200–255, the red channel to 254–255 and the green channel to 170–255. The threshold was then set at 20 and the image saved as a TIFF file. Images were imported into ImageJ and eggs were quantified using the particle counting function. Particle size and shape parameters were based on the values obtained in morphometric studies, and chosen to discriminate between bona fide strongyle eggs and other chitin-containing objects that might be present in the faeces such as yeast, fungi and their spores, and ingested arthropod fragments. Only particles whose areas were between 65 and 140 pixels were counted, corresponding to an area

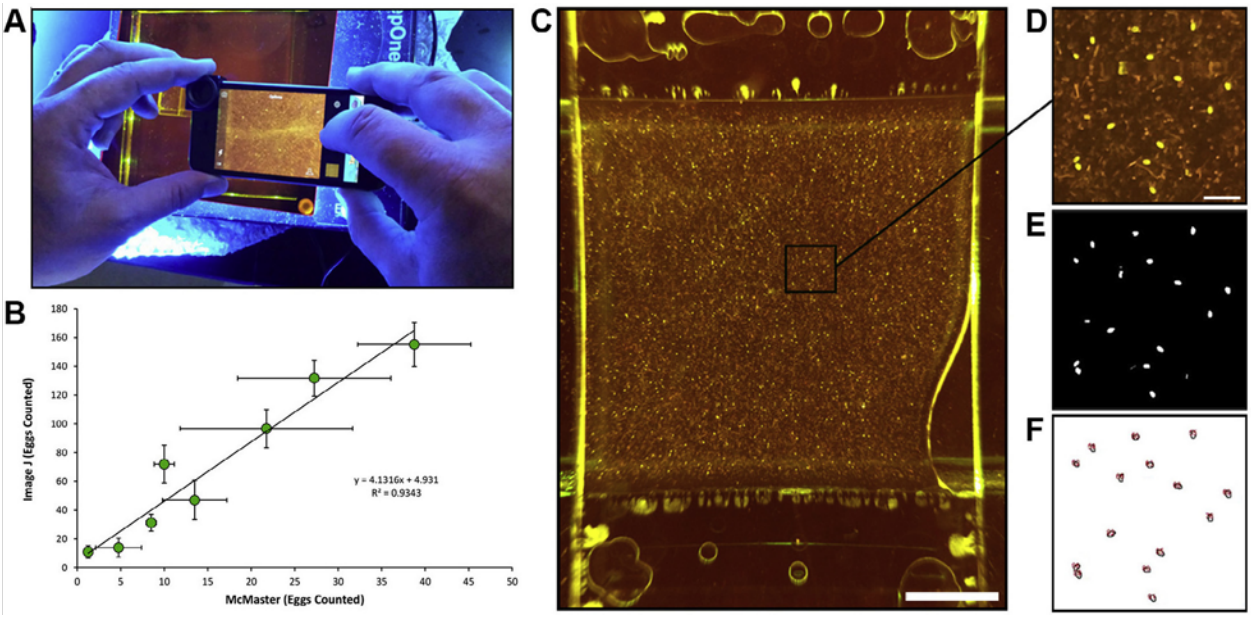

Fig. 1. Imaging and computational enumeration of strongyle eggs in equine faeces in a McMaster chamber using a cellular phone. (A) Illustration of experimental imaging set-up using a McMaster chamber placed in a fluorescent gel imager and an Apple iPhone 5s with an accessory macroscopic lens. (B) Comparison of egg counts obtained from eight different equine faecal samples using manual McMaster counting and the automated system. Data points show ± S.D. (n = 4). (C) Example of a whole-field image of a sample in a McMaster chamber. Scale bar = 4 mm. (D) Close-up view showing fluorescing strongyle eggs. Scale bar = 400 µm. (E) The same view as (D) after electronic thresholding to isolate eggs from the background. (F) The same view as (D) and (E), showing the eggs identified by the algorithm. Note that some of the thresholded particles in (E) have been excluded based on their shape and/or size.

Please cite this article in press as: Slusarewicz, P., et al. Automated parasite faecal egg counting using fluorescence labelling, smartphone image capture and computational image analysis. Int. J. Parasitol. (2016), http://dx.doi.org/10.1016/j.ijpara.2016.02.004

Table 1
Morphometric analysis of strongyle and ascarid eggs measured computationally by ImageJ software. Bright field or fluorescence images were produced of unstained and unbleached (native) or bleached and fluorescent-chitin binding domain stained eggs from the same faecal samples and various size and shape parameters determined. Data are presented as means ± S.D. Differences between untreated and treated eggs were all statistically significant ($P < 0.0001$) except for ascarid aspect ratio.

	Ascarids		Strongyles	
	Native ($n = 225$)	Bleached ($n = 157$)	Native ($n = 174$)	Bleached ($n = 362$)
Area (μm^2)	5704.3 ± 443.9	7125.8 ± 359.1	3953.2 ± 292.5	4444.1 ± 442.0
Aspect ratio	1.09 ± 0.05	1.10 ± 0.05	1.93 ± 0.16	1.73 ± 0.19
Major axis (μm)	89.1 ± 4.2	102.1 ± 3.4	98.5 ± 6.4	100.9 ± 9.5
Minor axis (μm)	81.5 ± 3.6	92.7 ± 3.2	51.1 ± 2.2	58.5 ± 2.6

range of approximately 2750–5900 μm^2 (based on a final resolution of 6.5 μm/pixel). Particles at the edges of the image were discarded and the results exported to a spreadsheet and sorted in ascending order by AR, defined as the ratio between the width and the length of the particle. Only particles with an AR between 1.3 and 2.6 were included in the analysis.

2.4.1. Egg morphometric analysis

Samples were collected from foals naturally infected with ascarid and strongyle parasites ($n = 10$). To both determine whether these eggs can be distinguished solely by computational morphometric criteria and to determine the values of such parameters, we photographed numerous fields of either untreated eggs floating in McMaster chambers under bright field illumination, or of bleached and fluorescently stained eggs using a fluorescence microscope.

2.4.2. Comparison of computer counts with manual McMaster

Because the McMaster FEC is the standard technique recommended by the WAAVP we used it as a comparator with the smartphone technology. To this effect, treated faeces were placed into a polycarbonate McMaster slide chamber and then a fluorescent gel imager, and photographed using an iPhone 5s fitted with a macro lens (Fig. 1A). The resulting image was transferred to a computer, the background was digitally removed (Fig. 1E), and particles counted using ImageJ software (NIH). Eggs were identified based on surface area and AR (Fig. 1F) using values derived from the measurements described above. McMaster egg counts were generated using a standard version of the technique (Roepstorff and Nansen, 1998) with a detection limit of 50 eggs per gram of faeces (EPG) and using saturated glucose-salt as flotation medium (specific gravity of 1.26). For this study, eight equine samples containing strongyle eggs were analysed using both methods.

2.4.3. Comparison of in-phone with manual McMaster counts

We built three units using smartphones with increasingly higher resolution sensors but the same optical magnification to assess the effect of pixel number on effective magnification. The three smartphones utilised were the iPhone 5s (8 megapixel (MP) camera), the Sony Experia Z3 (20 MP), and the Nokia Lumia (38 MP). Scale bars for output images were drawn using the stainless steel support mesh which was visible under the nylon capture filter as a reference, and whose aperture size was 250 μm. We chose the iPhone 5s unit (Fig. 2A–E) as a worst-case scenario to assess system performance and produced a custom application so that enumeration could be accomplished by the phone in situ.

In the case of in-phone counting, a curves adjustment function and the ImageJ particle counting algorithms were incorporated into an app on the smartphone itself. In this case, curve settings were 160–161 for RGB, 254–255 for the red channel and 254–255 for the blue channel. No other thresholding filters were applied. Egg shape parameters for strongyles were: size = 55–130 and AR = 1.3–2.5. For ascarids parameters were: size = 130–200 and AR = 1–1.3.

2.4.3.1. Imaging in McMaster chambers. In the first study using the iPhone in conjunction with the PrepOne Sapphire unit, eight individual equine faecal samples in flotation solution and containing only strongyle eggs with counts ranging from approximately 60–2200 EPG were processed both by the classical McMaster method (Roepstorff and Nansen, 1998) and the new method described. In each case, four aliquots of slurry from each sample were processed and counted.

2.4.3.2. Imaging directly on a membrane filter. Five individual equine faecal samples in flotation solution and containing only strongyle eggs with counts ranging from approximately 250–2000 EPG were processed both by the classical McMaster method described in previous sections and the automated smartphone method (Fig. 2A–D). Furthermore, a dilution series was created from one equine sample containing 1916 strongyle EPG, as assessed by traditional McMaster egg-counting by loading between 0.1 and 0.6 g of faeces into the system. Counts were generated as described in Section 2.4.3.

2.4.3.3. Differentiation of strongyle and ascarid eggs. In the case of the ascarid/strongyle mixture, the sample was processed as described for the above filter study but the sample was bleached for 5 min instead of 1 min in order to expose the chitin in the ascarid egg shells. Four replicates of the pooled slurry were counted by the manual McMaster method and the automated system. Ascarid:strongyle ratios were computed by calculating the average ratio for each combination of four counts conducted for each method (i.e. 16 variations).

2.5. Statistical analyses

Correlation between the mean results from the two counting methods was determined using least square means regression. The difference between the counts generated by the two methods was analysed with a dependent group *t*-test using the *t*-test procedure in SAS (version 9.3, SAS Institute, Cary, NC, USA). Egg count data were log-transformed to achieve normal distribution where needed. All statistical analyses were interpreted at the $\alpha = 0.05$ level.

The ascarid/strongyle differential counts were analysed statistically with SAS software using mixed linear models for differences between egg counts generated for each egg type (ascarid and strongyle) between the two methods. The 'mixed' procedure was used with count number as a random effect. Method and egg type were kept as class variables, while the egg count generated was considered continuous. Egg count data were log-transformed to achieve normal distribution where needed. Furthermore, difference between ascarid:strongyle ratios generated with the two egg counting methods were analysed with an independent group *t*-test using the *t*-test procedure in SAS.

Please cite this article in press as: Slusarewicz, P., et al. Automated parasite faecal egg counting using fluorescence labelling, smartphone image capture and computational image analysis. Int. J. Parasitol. (2016), http://dx.doi.org/10.1016/j.ijpara.2016.02.004

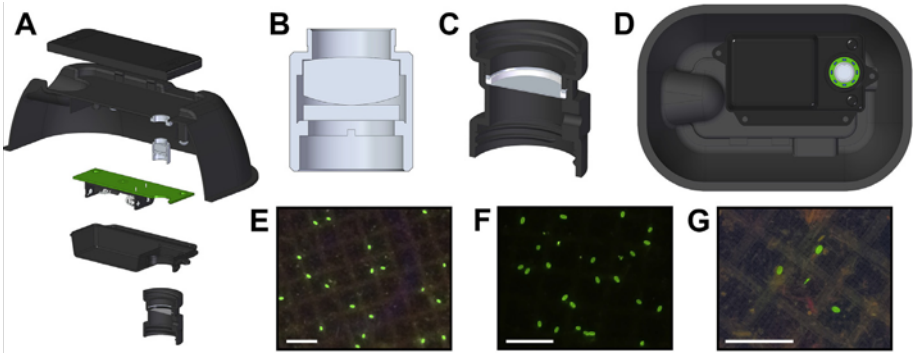

Fig. 2. Epifluorescene imaging device for smartphones and sample images. (A) Cutaway illustration showing, from top to bottom, cellular phone, external housing, optical tube, circuit board for light emitting diodes, circuit board cover and sample filter. (B) Cross section of the optical tube showing positioning of the adaptive lens above the emission filter. (C) Cross section of the filter unit consisting of two screwed-together halves, sandwiching the egg-capturing filter. (D) Underside view showing the circuit board cover in place and the arrangement of the light emitting diodes. (E, F) Images of stained fluorescing equine strongyles in faeces, captured using units built for the Apple iPhone 5s (8 megapixel), Sony Experia Z3 (20 megapixel) and Nokia Lumia 1020 (38 megapixel) cellular phones, respectively. (Scale bar = 500 μm).

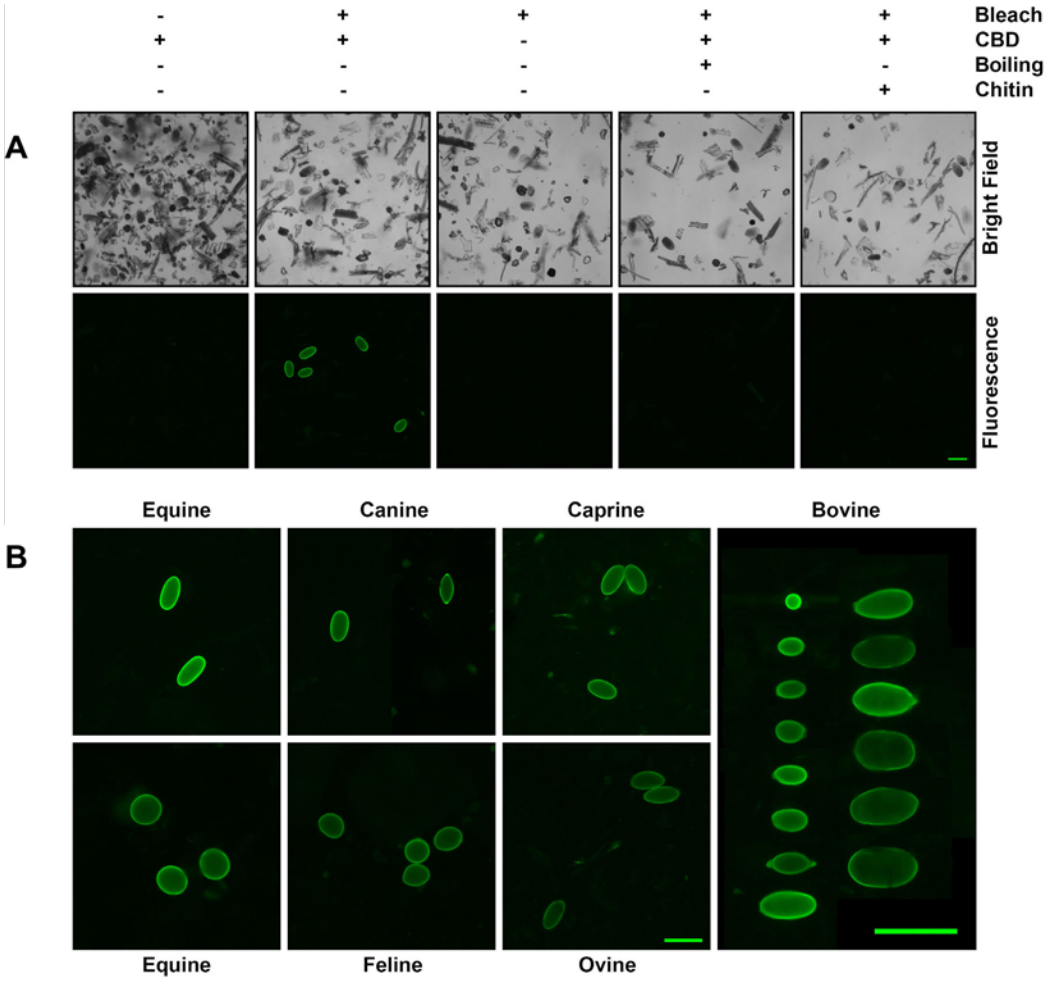

Fig. 3. Fluorescent staining of parasite eggs in faeces using the chitin binding domain. (A) Bright-field and corresponding fluorescence images of strongyle eggs in untreated equine faeces, bleached and stained faeces, bleached only faeces, bleached faeces stained with boiled fluorescent-chitin binding domain and bleached faeces stained with fluorescent-chitin binding domain pre-treated with chitin hydrolysate. Scale bar = 100 μm. (B) A variety of parasite eggs stained in the faeces of various mammalian species, namely equine strongles (upper image) and ascarids (lower image), canine hookworm (strongyle) and *Trichuris vulpis* (composite image), feline *Toxocara cati*, caprine and ovine trichostrongyles, and a composite image of a number of parasite eggs in a single bovine sample including *Nematodirus* spp., trichostrongyles, *Trichuris* spp. and coccidian oocysts. Scale bars = 100 μm (equine through ovine) and 200 μm (bovine).

Please cite this article in press as: Slusarewicz, P., et al. Automated parasite faecal egg counting using fluorescence labelling, smartphone image capture and computational image analysis. Int. J. Parasitol. (2016), http://dx.doi.org/10.1016/j.ijpara.2016.02.004

3. Results

3.1. Egg staining

We produced a recombinant version of the CBD of chitinase A1 from *B. circulans*. Initial attempts to stain strongyle eggs failed (Fig. 3A, however bleaching the faecal samples led strongyle eggs to fluoresce intensely upon F-CBD treatment with little staining observed in the copious extraneous faecal debris (Fig. 3A). Bleaching did not induce egg autofluorescence since eggs in bleached, unstained faeces did not fluoresce, and binding was specific because boiled F-CBD and F-CBD pretreated with a chitin hydrolysate both failed to stain eggs.

F-CBD stained eggs, in bleached faeces from multiple mammalian species (Fig. 3B), including equine strongyles and *Parascaris* spp. (ascarid), caprine and ovine trichostrongyles, canine strongyles (hookworm) and *Trichuris vulpis* (whipworm), feline *Toxocara cati* (ascarid) and a variety of eggs in bovine faeces including *Nematodirus* spp., trichostrongyles and *Trichuris* spp., and coccidian oocysts. Staining of *Trichuris* eggs was striking because F-CBD bound to both the shell and the operculae.

Most eggs required just 1 min of bleaching, but the thick proteinaceous coat of equine ascarids required 5 min. Surprisingly, the smooth shell of *Trichuris* eggs also required a 5 min bleach, although the operculae stained after only 1 min (not shown). Bleaching also reduced the amount of faecal debris on the filter and rendered it more translucent, thereby reducing its propensity to mask eggs.

3.2. Egg morphometric analysis

Fluorescent ascarid and strongyle eggs could be distinguished by surface area (Fig. 4A) and AR (Fig. 4B) as well as minor, but not major, axis (Table 1). We chose to utilise both surface area and AR as parameters to not only distinguish the two egg types from one another but also from other chitin-containing components possibly present in the faeces.

Bleaching and staining increased the size of both ascarid and strongyle eggs (Table 1). Ascarid egg area increased by 25% due to enlargement of the major and minor axes by 14.6 and 13.7%, respectively. Strongyle egg area increase was half that of ascarids (12.4%) while the minor axis length increased more than the major at 14.5% versus 2.4%. The similar biaxial enlargement of ascarid eggs resulted in no change in aspect ratio, while the preferential transverse expansion of strongyle eggs resulted in an average aspect ratio decrease of 11.4%. All of these changes were statistically significant ($P < 0.0001$).

The morphometric changes were not artefacts from using two different imaging modes because fluorescent images overlaid their bright field counterparts exactly (Supplementary Fig. S1). Graphs of the changes in each parameter frequency distribution for each egg type are shown in Supplementary Figs. S2 and S3.

3.3. Imaging in McMaster chambers

Fluorescing eggs could be easily discerned from the background faecal material (Fig. 1C, D), and particles corresponding to autofluorescing background or extraneous chitin-containing material were not counted (cf. Fig. 1E, F).

Comparison of this automated method with manual McMaster counting resulted in a significant correlation ($R^2 = 0.93$; Fig. 1B). Due to the concentration of eggs during filtration, the automated system detected significantly more eggs ($P = 0.0082$) with significantly smaller variance ($P = 0.0011$) than the McMaster method. The slope of the line of best fit was 4.13, but because 10 times more material was loaded into the capture filter in the automated method than the McMaster chamber in the manual method, this represented an egg yield of 41%.

3.4. Imaging on filters

The Sony Experia Z3 (20 MP) produced larger egg images than the iPhone 5s (8 MP) but was out-performed by the Nokia Lumia 1020 (38 MP) (Fig. 2E–G).

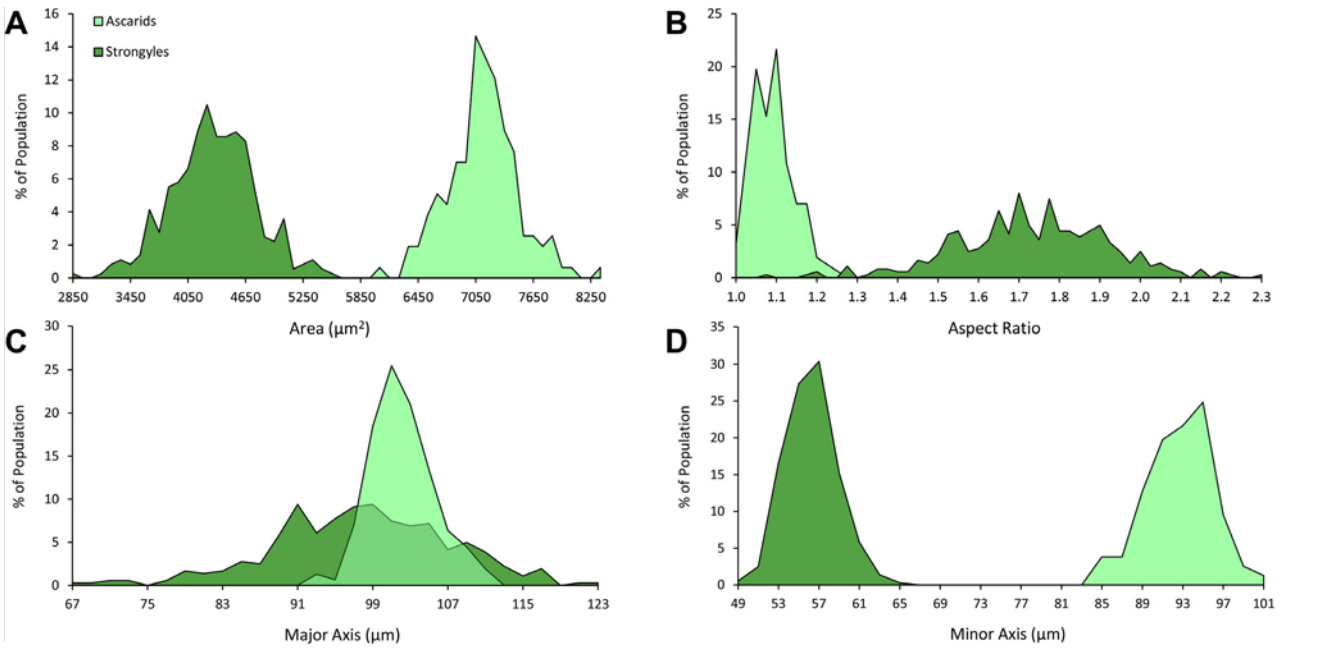

Fig. 4. Size and shape distribution of bleached, stained ascarid and strongyle eggs. Ascarid or strongyle egg-containing faecal samples were bleached and stained with fluorescent-chitin binding domain, photographed using a fluorescence microscope, and measured using ImageJ software (ascarids $n = 157$, strongyles $n = 362$). Frequency distributions of surface areas (A), aspect ratios (B), and major (C) and minor (D) axes for both egg types are shown.

Please cite this article in press as: Slusarewicz, P., et al. Automated parasite faecal egg counting using fluorescence labelling, smartphone image capture and computational image analysis. Int. J. Parasitol. (2016), http://dx.doi.org/10.1016/j.ijpara.2016.02.004

The dose response of strongyle egg-containing faeces from the same sample was linear (R^2 = 0.996) (Fig. 5A). The line slope was 1323 EPG, corresponding to a recovery of 69%, substantially higher than previously. After accounting for the fact that the imaging unit prototype only captured 87% of the surface of the circular filter, this recovery rose to 79%.

The comparison with McMaster egg counts produced an improved correlation (R^2 = 0.98) compared with the previous system (cf. Figs. 1B and 5B). Once again, many more eggs (12.5×, from the slope of the line) were counted by the automated system due to the larger amount of faecal material (20×) available for analysis, indicating a substantial increase in sensitivity. After accounting for the non-imaged filter area, the egg yield of the automated system was 72%.

The relative standard deviations (%RSDs) of the values generated by the automated system were significantly lower (P = 0.0177) than the manual McMaster method (Fig. 5C), indicating higher diagnostic precision.

3.5. Differentiation of ascarid and strongyle eggs

We confirmed microscopically that a sample containing both ascarid and strongyle type eggs could indeed be treated such that both were labelled (Fig. 5D) and identified based on the thresholds defined in the smartphone application (Fig. 5E). Due to increased loading, the automated system enumerated significantly more eggs (12.8× and 13.9× for strongyles (P < 0.0001) and ascarids (P < 0.0001), respectively (Fig. 5F)), corresponding to recoveries of 73.6% and 79.9%, and the %RSD was 10 and four times lower for strongyles and ascarids, respectively (4.1% versus 40.1% for strongyles and 4.9% versus 22.4% for ascarids). We calculated ascarid:strongyle ratios (ASRs) for each of the 16 possible combinations of the quadruplicate counts for each method (Fig. 5G). The mean manual McMaster ASR was 1.33 compared with 1.28 for the automated method. This difference was not statistically significant (P = 0.7283), indicating that the automated method discriminated between egg types as well as the manual method. As was the case for egg counts, the %RSD of the manual McMaster ratio was significantly larger (45.3%) than the automated smartphone system (5.7%) (P < 0.0001).

4. Discussion

We have, to our knowledge, described the first smartphone-based parasite faecal egg counting technique. The ability of F-CBD to stain all the eggs tested to date across many disparate parasite genera collected from different mammalian species suggests that chitin is indeed a tractable UEM. The constructed system is capable of generating a quantitative measure of the amount of eggs in a faecal sample, and we have demonstrated its ability to differentiate between the two most clinically important egg types present in equine faeces. Due to the ability to load more faecal material, both automated methods described here counted more eggs than the standard McMaster procedure for any given faecal sample. In the case of imaging in McMaster chambers the ~40% recovery may in part have been due to inefficient harvesting by manual pipetting from the capture filter, and this is consistent with the elevated recovery, when imaging directly on the filter for both strongyle and ascarid eggs, of between 70% and 80%. Egg loss in the direct filter imaging method is probably due to a combination of a number of factors such as: (i) some eggs are not counted by the current algorithms (Fig. 5E, arrowheads) because some smaller eggs lie close to the size threshold used to discriminate them from smaller irrelevant particles, and because some do not stain as brightly as others and may be eliminated by the digital thresholding; (ii) eggs at the edges of the filter tend to be distorted due to lens aberrations and are sometimes ignored; (iii) a small number of eggs are presumably lost due to burial by the faecal particulates present on the capturing filter; and (iv) two adjacent, touching eggs are counted as a single particle or ignored. Despite these challenges, the automated method in the current form still substantially out-performs the most recommended egg-counting method in use in veterinary practice today, and we are working to maximise yields by improving both optics and algorithms.

The process described here can be conducted in 4–9 min depending on the bleaching duration. In comparison, one recent

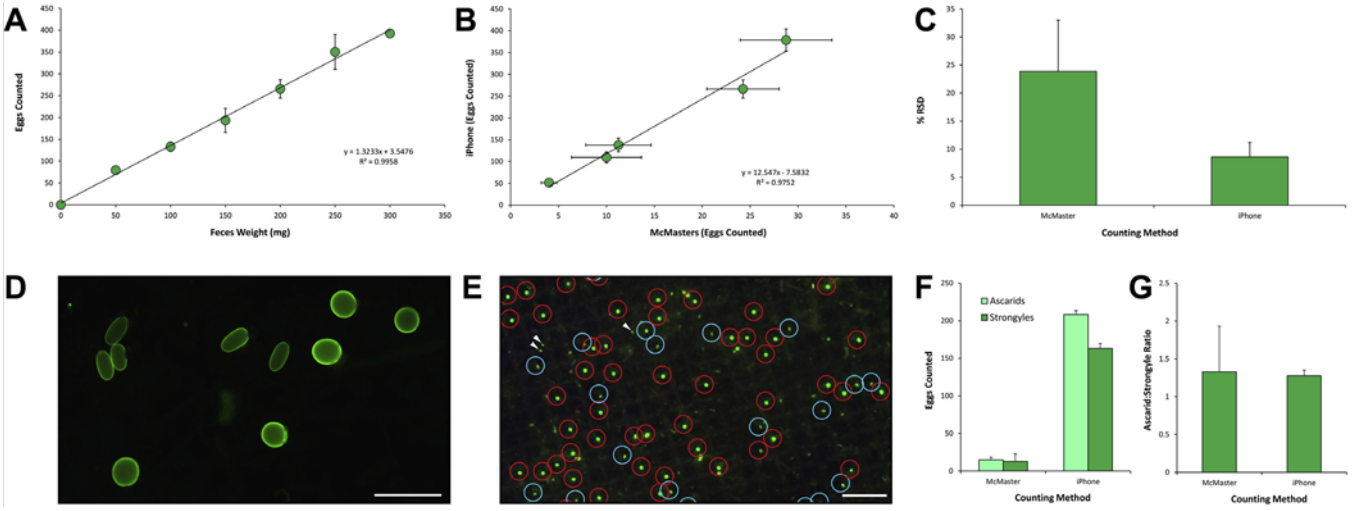

Fig. 5. Performance evaluation of the Apple iPhone 5s epifluorescence device and built-in image analysis application. (A) Dose response of automated counting as assessed by increasing the amount of faeces loaded onto the filter. Data points show ± S.D. (n = 3). (B) Comparison of egg counts obtained from five different equine faecal samples using manual McMaster counting and the automated system. Data points show ± S.D. (n = 4). (C) Mean percentage of relative standard deviation for manual and automated counts in (B), shown ± S.D. (n = 5). (D) Fluorescence microscope image of mixed strongyle/ascarid equine stained faecal sample used to test shape discrimination. (E) Example of output from iPhone application show identified strongyles (blue circles), ascarids (red circles) and uncounted strongyles (white arrowheads). (F) Results of automated and manual counts of the mixed egg-type faecal sample. Data points show ± S.D. (n = 4). (G) Mean ascarid:strongyle ratios for automated and manual counts. Data points show ± S.D. (n = 16). Scale bars = 200 μm (D) and 1000 μm (E).

Please cite this article in press as: Slusarewicz, P., et al. Automated parasite faecal egg counting using fluorescence labelling, smartphone image capture and computational image analysis. Int. J. Parasitol. (2016), http://dx.doi.org/10.1016/j.ijpara.2016.02.004

study (Barda et al., 2014) estimated the processing time for McMaster strongyle counts is 7 min per sample, whereas one of the most common techniques in human parasitology, the Kato-Katz, took 48 min per sample. These estimates, however, did not include the time taken to transport samples to a laboratory, nor consider that manual counting is a rate limiting step that must be conducted in series for multiple samples. This is eliminated by parallel processing because samples that are stained in parallel can be counted almost instantaneously, further reducing the time required per test. In our hands we could stain and count four strongyle-containing samples in less than 10 min, compared with the 20–25 min that would be required for the McMaster method. Automation of the staining process could potentially further increase the throughput of the system. These improvements in efficiency, coupled to the superior sensitivity and precision reported here, makes this a significant improvement over current methodologies.

The smartphone unit also offers practical advantages over existing egg count techniques. First, it obviates the need for a laboratory microscope and an experienced technician. Second, it does not require access to an electrical outlet, as it runs on batteries, and is thus amenable for remote field work, where fresh samples can be processed rather than having to be preserved in formalin for later laboratory analysis. In this regard, our simple syringe-driven filtration system can be manually operated and requires no power, while our preliminary experiments suggest that F-CBD is stable for at least 1 week at 37 °C and may not require refrigerated transportation to remote undeveloped areas. Furthermore, the image can be saved after capture and stored as a permanent data record, and can be reanalysed if needed, providing yet another advantage over traditional methods. This image can also be useful as a means to facilitate communication of test results and associated recommendations to clients and patients. Thus, this technology overcomes significant obstacles to adopting surveillance-based parasite control strategies by making egg counts easier to obtain in a real-time setting.

Acknowledgements

This work was partially funded by an Small Business Innovation Research grant from the United States Department of Agriculture, USA (#2015-33610-23497; P.S.) and by grants from MEP Equine Solutions, LLC, USA, (M.K.N.). CBD protein production was supported in part by the UK COBRE Center for Molecular Medicine Protein and Molecular Technologies cores (which are supported in part by National Institutes of Health, USA, Grant Number P20GM110787; G.P., K.M.C., M.M., and D.W.R. and National Science Foundation, USA, Grant IIA-1355438; D.W.R). We thank Eric Hauck, David Ward, Ellie Hawes and Winston Walker for their assistance in designing and building the imaging units, and Richard Chan for his suggestion of using a cell phone and the Sapphire PrepOne for imaging eggs in McMaster chambers.

Appendix A. Supplementary data

Supplementary data associated with this article can be found, in the online version, at http://dx.doi.org/10.1016/j.ijpara.2016.02.004.

References

Alum, A., Rubino, J.R., Ijaz, M.K., 2010. The global war against intestinal parasites – should we use a holistic approach? Int. J. Infect. Dis. 14, e732–e738.

Barda, B.D., Rinaldi, L., Ianniello, D., Zepherine, H., Salvo, F., Sadutshang, T., Cringoli, G., Clementi, M., Albonico, M., 2013. Mini-FLOTAC, an innovative direct diagnostic technique for intestinal parasitic infections: experience from the field. PLoS Negl. Trop. Dis. 7, e2344.

Barda, B., Cajal, P., Villagran, E., Cimino, R., Juarez, M., Krolewiecki, A., Rinaldi, L., Cringoli, G., Burioni, R., Albonico, M., 2014. Mini-FLOTAC, Kato-Katz and McMaster: three methods, one goal; highlights from north Argentina. Parasit. Vectors 7, 271.

Bird, A.F., McClure, M.A., 1976. The tylenchid (Nematoda) egg shell: structure, composition and permeability. Parasitology 72, 19–28.

Bogoch, I.I., Andrews, J.R., Speich, B., Utzinger, J., Ame, S.M., Ali, S.M., Keiser, J., 2013. Short report: mobile phone microscopy for the diagnosis of soil-transmitted helminth infections: a proof-of-concept study. Am. J. Trop. Med. Hyg. 88, 626–629.

Bogoch, I.I., Sayasone, S., Vonghachack, Y., Meister, I., Utzinger, J., Odermatt, P., Andrews, J.R., Keiser, J., 2016. Diagnosis of *Opisthorchis viverrini* infection with handheld microscopy in Lao People's Democratic Republic. Am. J. Trop. Med. Hyg. 94, 158–160.

Burgwyn, B., Nagel, B., Ryerse, J., Bolla, R.I., 2003. Heterodera glycines: eggshell ultrastructure and histochemical localization of chitinous components. Exp. Parasitol. 104, 47–53.

Castanon, C.A.B., Fraga, J.S., Fernandez, S., Gruber, A., Costa, L.D., 2007. Biological shape characterization for automatic image recognition and diagnosis of protozoan parasites of the genus *Eimeria*. Pattern Recogn. 40, 1899–1910.

Cezar, A.S., Toscan, G., Camillo, G., Sangioni, L.A., Ribas, H.O., Vogel, F.S., 2010. Multiple resistance of gastrointestinal nematodes to nine different drugs in a sheep flock in southern Brazil. Vet. Parasitol. 173, 157–160.

Cooke, I.R., Laing, C.J., White, L.V., Wakes, S.J., Sowerby, S.J., 2015. Analysis of menisci formed on cones for single field of view parasite egg microscopy. J. Microsc. 257, 133–141.

Cringoli, G., Rinaldi, L., Veneziano, V., Capelli, G., Scala, A., 2004. The influence of flotation solution, sample dilution and the choice of McMaster slide area (volume) on the reliability of the McMaster technique in estimating the faecal egg counts of gastrointestinal strongyles and *Dicrocoelium dendriticum* in sheep. Vet. Parasitol. 123, 121–131.

Cringoli, G., Rinaldi, L., Maurelli, M.P., Utzinger, J., 2010. FLOTAC: new multivalent techniques for qualitative and quantitative copromicroscopic diagnosis of parasites in animals and humans. Nat. Protoc. 5, 503–515.

da Cruz, D.G., da Rocha, L.O., Arruda, S.S., Palieraqui, J.G., Cordeiro, R.C., Santos Jr., E., Molento, M.B., Santos, C.P., 2010. Anthelmintic efficacy and management practices in sheep farms from the state of Rio de Janeiro, Brazil. Vet. Parasitol. 170, 340–343.

Dogantekin, E., Yilmaz, M., Dogantekin, A., Avci, E., Sengur, A., 2008. A robust technique based on invariant moments – ANFIS for recognition of human parasite eggs in microscopic images. Expert Syst. Appl. 35, 728–738.

Ephraim, R.K.D., Duah, E., Cybulski, J.S., Prakash, M., D'Ambrosio, M.V., Fletcher, D.A., Keiser, J., Andrews, J.R., Bogoch, I.I., 2015. Diagnosis of *Schistosoma haematobium* infection with a mobile phone-mounted foldscope and a reversed-lens cell scope in Ghana. Am. J. Trop. Med. Hyg. 92, 1253–1256.

Ghazali, K.H., Hadi, R.S., Mohamed, Z., 2013. Automated system for diagnosis intestinal parasites by computerized image analysis. Mod. Appl. Sci. 7, 98–114.

Gordon, H.M., Whitlock, H.V., 1939. A new technique for counting nematode eggs in sheep faeces. J. Counc. Sci. Ind. Res. 12, 52.

Howell, S.B., Burke, J.M., Miller, J.E., Terrill, T.H., Valencia, E., Williams, M.J., Williamson, L.H., Zajac, A.M., Kaplan, R.M., 2008. Prevalence of anthelmintic resistance on sheep and goat farms in the southeastern United States. J. Am. Vet. Med. Assoc. 233, 1913–1919.

Kaplan, R.M., 2004. Drug resistance in nematodes of veterinary importance: a status report. Trends Parasitol. 20, 477–481.

Kenyon, F., Greer, A.W., Coles, G.C., Cringoli, G., Papadopoulos, E., Cabaret, J., Berrag, B., Varady, M., Van Wyk, J.A., Thomas, E., Vercruysse, J., Jackson, F., 2009. The role of targeted selective treatments in the development of refugia-based approaches to the control of gastrointestinal nematodes of small ruminants. Vet. Parasitol. 164, 3–11.

Leathwick, D.M., Besier, R.B., 2014. The management of anthelmintic resistance in grazing ruminants in Australasia – strategies and experiences. Vet. Parasitol. 204, 44–54.

Levecke, B., Rinaldi, L., Charlier, J., Maurelli, M.P., Bosco, A., Vercruysse, J., Cringoli, G., 2012. The bias, accuracy and precision of faecal egg count reduction test results in cattle using McMaster, Cornell-Wisconsin and FLOTAC egg counting methods. Vet. Parasitol. 188, 194–199.

Linder, E., Grote, A., Varjo, S., Linder, N., Lebbad, M., Lundin, M., Diwan, V., Hannuksela, J., Lundin, J., 2013. On-chip imaging of *Schistosoma haematobium* eggs in urine for diagnosis by computer vision. PLoS Negl. Trop. Dis. 7, e2547.

Mes, T.H., Eysker, M., Ploeger, H.W., 2007. A simple, robust and semi-automated parasite egg isolation protocol. Nat. Protoc. 2, 486–489.

Nielsen, M.K., Pfister, K., von Samson-Himmelstjerna, G., 2014. Selective therapy in equine parasite control – application and limitations. Vet. Parasitol. 202, 95–103.

Olson, S.K., Greenan, G., Desai, A., Muller-Reichert, T., Oegema, K., 2012. Hierarchical assembly of the eggshell and permeability barrier in *C. elegans*. J. Cell Biol. 198, 731–748.

Peregrine, A.S., Molento, M.B., Kaplan, R.M., Nielsen, M.K., 2014. Anthelmintic resistance in important parasites of horses: does it really matter? Vet. Parasitol. 201, 1–8.

Perry, R.N., Trett, M.W., 1986. Ultrastructure of the eggshell of *Heterodera schachtii* and *H. glycines* (Nematoda: Tylenchida). Revue Nematol., 399–403

Quiles, F., Balandier, J.Y., Capizzi-Banas, S., 2006. In situ characterisation of a microorganism surface by Raman microspectroscopy: the shell of *Ascaris* eggs. Anal. Bioanal. Chem. 386, 249–255.

Robert, M., Nielsen, M.K., Stowe, C.J., 2015. Attitudes towards implementation of surveillance-based parasite control on Kentucky Thoroughbred farms – current strategies, awareness, and willingness-to-pay. Equine Vet. J. 47, 694–700.

Roepstorff, A., Nansen, P., 1998. Epidemiology, diagnosis and control of helminth parasites of swine. In: FAO Animal Health Manual. United Nations Food and Agriculture Organization, Rome.

Sowerby, S.J., Crump, J.A., Johnstone, M.C., Krause, K.L., Hill, P.C., 2016. Smartphone microscopy of parasite eggs accumulated into a single field of view. Am. J. Trop. Med. Hyg. 94, 227–230.

Stoll, N.R., 1930. On methods of counting nematode ova in sheep dung. Parasitology 22, 116–136.

Suzuki, C.T.N., Gomes, J.F., Falcao, A.X., Papa, J.P., Hoshino-Shimizu, S., 2013. Automatic segmentation and classification of human intestinal parasites from microscopy images. IEEE Trans. Biomed. Eng. 60, 803–812.

Vadlejch, J., Petrtyl, M., Zaichenko, I., Cadkova, Z., Jankovska, I., Langrova, I., Moravec, M., 2011. Which McMaster egg counting technique is the most reliable? Parasitol. Res. 109, 1387–1394.

Vercruysse, J., Albonico, M., Behnke, J.M., Kotze, A.C., Prichard, R.K., McCarthy, J.S., Montresor, A., Levecke, B., 2011. Is anthelmintic resistance a concern for the control of human soil-transmitted helminths? Int. J. Parasitol. Drugs. Drug Resist. 1, 14–27.

Vercruysse, J., Levecke, B., Prichard, R., 2012. Human soil-transmitted helminths: implications of mass drug administration. Curr. Opin. Infect. Dis. 25, 703–708.

Wharton, D.A., 1983. The production and functional morphology of helminth egg-shells. Parasitology 86 (Pt 4), 85–97.

WHO, 2006. Preventive Chemotherapy in Human Helminthiasis – Coordinated Use of Anthelminthic Drugs in Control Interventions: A Manual for Health Professionals and Programme Managers. World Health Organization, Geneva, Switzerland.

Wood, I.B., Amaral, N.K., Bairden, K., Duncan, J.L., Kassai, T., Malone Jr., J.B., Pankavich, J.A., Reinecke, R.K., Slocombe, O., Taylor, S.M., 1995. World Association for the Advancement of Veterinary Parasitology (W.A.A.V.P.) second edition of guidelines for evaluating the efficacy of anthelmintics in ruminants (bovine, ovine, caprine). Vet. Parasitol. 58, 181–213.

Yang, Y.S., Park, D.K., Kim, H.C., Choi, M.H., Chai, J.Y., 2001. Automatic identification of human helminth eggs on microscopic fecal specimens using digital image processing and an artificial neural network. IEEE Trans. Biomed. Eng. 48, 718–730.

Zhang, Y., Foster, J.M., Nelson, L.S., Ma, D., Carlow, C.K., 2005. The chitin synthase genes chs-1 and chs-2 are essential for *C. elegans* development and responsible for chitin deposition in the eggshell and pharynx, respectively. Dev. Biol. 285, 330–339.

Zhu, H., Isikman, S.O., Mudanyali, O., Greenbaum, A., Ozcan, A., 2013. Optical imaging techniques for point-of-care diagnostics. Lab Chip 13, 51–67.

Please cite this article in press as: Slusarewicz, P., et al. Automated parasite faecal egg counting using fluorescence labelling, smartphone image capture and computational image analysis. Int. J. Parasitol. (2016), http://dx.doi.org/10.1016/j.ijpara.2016.02.004